analytical chemistry

Article

Cite This: *Anal. Chem.* 2019, 91, 10532−10540

pubs.acs.org/ac

Sequential Detection of Lipids, Metabolites, and Proteins in One Tissue for Improved Cancer Differentiation Accuracy

Haiyan Lu,[†] Hua Zhang,[†] Konstantin Chingin,[‡] Yiping Wei,[§] Jiaquan Xu,[‡] Mufang Ke,[†] Keke Huang,[†] Shouhua Feng,*[,†] and Huanwen Chen*[,‡]

[†]State Key Laboratory of Inorganic Synthesis and Preparative Chemistry, College of Chemistry, Jilin University, Changchun 130012, P. R. China

[‡]Jiangxi Key Laboratory for Mass Spectrometry and Instrumentation, East China University of Technology, Nanchang 330013, P. R. China

[§]Second Affiliated Hospital of Nanchang University, Nanchang 330006, P. R. China

Supporting Information

ABSTRACT: Traditionally, molecular information on metabolites, lipids, and proteins is collected from separate individual tissue samples using different analytical approaches. Herein a novel strategy to minimize the potential material losses and the mismatch between metabolomics, lipidomics, and proteomics data has been demonstrated based on internal extractive electrospray ionization mass spectrometry (iEESI-MS). Sequential detection of lipids, metabolites, and proteins from the same tissue sample was achieved without sample reloading and hardware alteration to MS instrument by sequentially using extraction solutions with different chemical compositions. With respect to the individual compound class analysis, the sensitivity, specificity, and accuracy obtained with the integrative information on metabolites, lipids, and proteins from 57 samples of 13 patients for lung cancer prediction was substantially improved from 54.0%, 51.0%, and 76.0% to 100.0%, respectively. The established method is featured by low sample consumption (ca. 2.0 mg) and easy operation, which is important to minimize systematic errors in precision molecular diagnosis and systems biology studies.

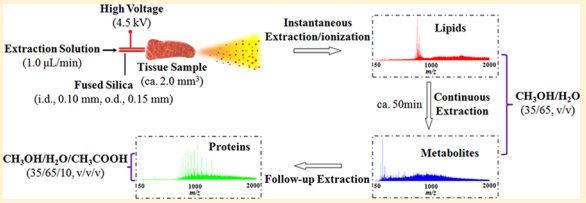

Biological tissue, which is intermediate between a single cell and a whole organism, is widely used in systems biology studies and molecular diagnosis.[1,2] Systematic bias, particularly among the results of metabolomics, lipidomics, and proteomics analyses, may occur in conventional omics approaches because different loci of tissue samples are analyzed.[2,3] Futher bias between the metabolomics, lipidomics, and proteomics data may be associated with the employment of different tissue samples and different analytical instruments. Logically, maintaining the instrumental conditions constant and recording different omics data using exactly the same piece of tissue sample should improve the accuracy and consistency of the analytical results. Therefore, it is of interest to implement and test an analytical strategy that could provide maximal molecular information from a single sample with the identical instrumental setup for systems biology studies.

Traditionally, the omics data on small metabolites, lipids, and proteins are separately collected using differential individual tissue samples by multiple analytical techniques, with cumbersome sample preparation steps including extraction, separation, and centrifugation, and a large amount of tissue samples required.[2,4,5] Statistics and bioinformatics tools are usually used to link the specific omics data to other systems biology information.[6] Yet, integrating multilayers of molecular information from different samples may smear the molecular profile of the individual samples, resulting in misleading conclusions owing to systematic errors caused by the nonhomologous samples. Direct profiling of small metabolites, lipids, and proteins from exactly the same sample minimizes the chance of material/information loss and system errors in systems biology studies, which may enable better mechanistic understanding of pathophysiological conditions, and thus leading to novel strategies for the early detection, prevention, and treatment of diseases with the improved accuracy of molecular diagnosis.[7,8]

Herein a novel strategy to minimize the potential material losses and the mismatch between metabolomics, lipidomics, and proteomics data has been demonstrated based on internal extractive electrospray ionization mass spectrometry (iEESI-MS). Sequential detection of lipids, metabolites, and proteins from exactly the same bulk tissue sample without sample reloading and hardware alteration to the MS instrument was achieved by sequentially applying extraction solutions with different chemical compositions. With respect to the individual compound class analysis, the sensitivity, specificity, and accuracy obtained with the integrative information on metabolites, lipids, and proteins from 57 samples of 13

Received: March 25, 2019
Accepted: July 16, 2019
Published: July 16, 2019

DOI: 10.1021/acs.analchem.9b01507
Anal. Chem. 2019, 91, 10532−10540

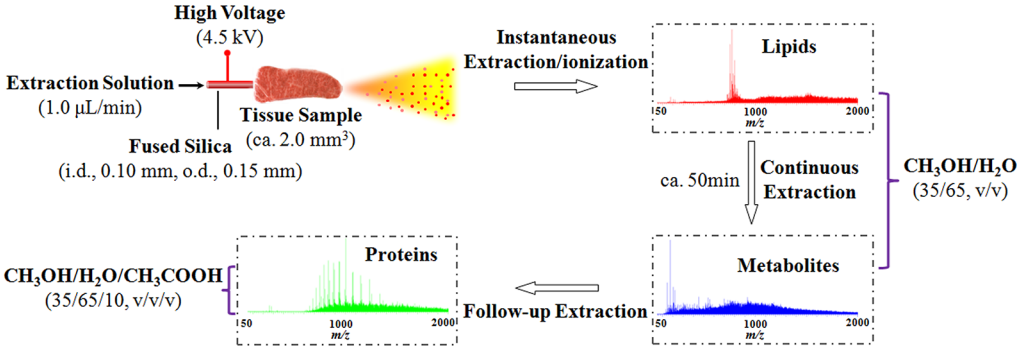

Figure 1. Schematic illustration of iEESI-MS for the sequential detection of lipids, small metabolites, and proteins in a single tissue sample.

patients for lung cancer prediction was substantially improved from 54.0%, 51.0%, and 76.0% to 100.0%, respectively. The established method is featured by low sample consumption (ca. 2.0 mg) and easy operation, which is important to minimize systematic errors in precision molecular diagnosis and systems biology studies.

EXPERIMENTAL SECTION

Materials and Reagents. The porcine lung samples were purchased from local meat stores. A total of 57 tissue samples (including 29 cancerous tissue samples and 28 normal tissue samples) from 13 patients were provided by the Second Affiliated Hospital of Nanchang University, with all the patients' informed consent. All the experiments were approved by the Medical Ethics Committee of the Hospital Institutional Review Board of the Second Affiliated Hospital of Nanchang University, and all clinical investigations were conducted according to the principles expressed in the Declaration of Helsinki.[9] All tissue samples were stored around −80 °C in a refrigerator. The fused capillary (i.d., 0.10 mm, o.d., 0.15 mm) was obtained from Agilent Technologies Co., Ltd. Methanol and acetic acid were HLPC grade and bought from ROE Scientific Inc. (Newark, U.S.A). The deionized water was provided by Milli-Q water purification system (Billerica, USA).

Instruments and Method. The iEESI-MS experiments[10−12] were carried out using a homemade iEESI ion source coupled with a linear trap quadruple (LTQ) mass spectrometer controlled by XCalibur 2.0 software (Thermo Scientific, San Jose, CA). Briefly, extraction solution (e.g., methanol/water/acetic acid) biased with high voltage was guided to flow through the tissue sample for extraction and electrospray ionization. In the current experimental approach, the sequential detection of lipids, small metabolites, and proteins from a single tissue sample (ca. 2.0 mm^3) was achieved in two stages. As shown in Figure 1, first, the extraction solution of CH_3OH/H_2O (v/v, 35/65) was employed for the iEESI-MS analysis, resulting in the instantaneous extraction/ionization of lipids, which was followed by the extraction/ionization of small metabolites after continuous infusion for ca. 30−80 min under the same experimental conditions. At last, the extraction solution was altered to $CH_3OH/H_2O/CH_3COOH$ (v/v/v, 35/65/10), and the extraction/ionization of proteins was enabled. For details about the iEESI-MS experiment and working conditions, refer to Supporting Information (Figure S1, S2 and S3).

Data Analysis. All raw data were processed through Soft Independent Modeling of Class Analogies (SIMCA) (version 13.0, Umetrics, Umeå, Sweden), Matlab (version 7.8.0, Mathworks, Inc., Natick, MA), R programming language (version 3.5.1), and SPSS (version 18.0, SPSS Inc., Chicago, IL, USA). First, the full scan MS data was exported to Microsoft Excel, which was arranged using the m/z value as independent variables and the signal intensity as dependent variables. Then, the exported MS data was mass realigned based on the m/z value in Matlab.[13] Next, the aligned data was used for orthogonal partial least-squares discriminant analysis (OPLS-DA) modeling in SIMCA and support vector machine (SVM) analysis in R, respectively. The OPLS-DA model goodness of fit was evaluated through three quantitative parameters (e.g., R^2X is the explained variation in X, R^2Y is the explained variation in Y, and Q^2Y is the predicted variation in Y).[14] In addition, permutation tests were performed with 200 iterations to validate the fitting quality of the model, and S-plots were constructed to screen potential biomarkers that contribute to the group differences. Total data were randomly divided into training sets and validation sets at the ratios of 7:3 in SVM analysis.

Pearson correlation analysis using SPSS 18.0 was conducted among the signal intensities of 19 signals with high variable influence on projection (VIP) value for the discrimination of cancerous and normal tissue samples, including small metabolites (e.g., m/z 147, 175, and 203) (VIP > 1.0), lipids (e.g., m/z 757, 773, 799, 825, and 849) (VIP > 1.0), and protein ions (e.g., m/z 758, 797, 842, 883, 891, 935, 947, 993, 1010, 1082, and 1165) (VIP > 5.0). All correlation coefficients calculated in SPSS were exported into Microsoft Excel, and further picture presentations were achieved by program in Matlab. Note that correlation analysis was only performed for the cancerous tissue samples.

RESULTS AND DISCUSSION

iEESI-MS. iEESI-MS directly characterizes the molecular information within the bulk sample without sample pretreatment.[10,11] Until now, iEESI-MS has been successfully applied in multidisciplines such as plant metabolomics (including direct molecular characterization of chemical compounds[10,12] as well as ongoing enzymatic reactions in plant tissue samples,[11] etc.), food science (including rapid screening of pork samples contaminated by β-agonists,[15] quantitative analysis various β-agonists in pork sample,[16] direct evaluation of metabolic effects of clenbuterol and salbutamol on pork quality,[17] identification of meat species based on hemoglobin,[18] and quantitative determination of fluoroquinolones from raw milk,[19] etc.), clinical analysis (including rapid discrimination of tissue samples of human esophageal squamous cell carcinoma,[12] lung cancer,[20] as well as endometriosis foci[21] and

DOI: 10.1021/acs.analchem.9b01507
Anal. Chem. 2019, 91, 10532−10540

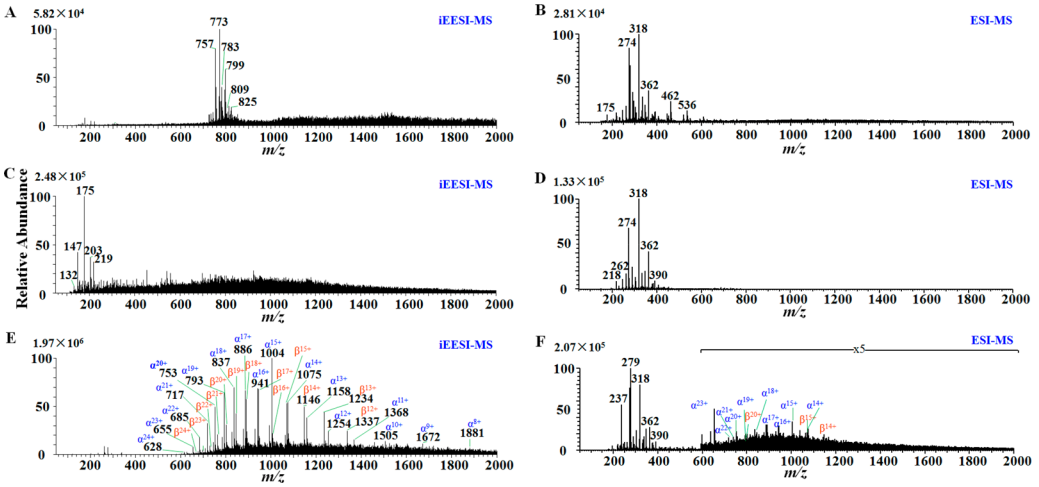

Figure 2. Comparative study of iEESI-MS and ESI-MS for the analysis of a single porcine lung tissue sample. (A) iEESI-MS spectrum obtained using CH_3OH/H_2O (v/v, 35/65) for 1 min; (B) ESI-MS spectrum of the extraction solution of porcine lung tissue obtained using CH_3OH/H_2O (v/v, 35/65) for 1 min; (C) iEESI-MS spectrum obtained using CH_3OH/H_2O (v/v, 35/65) for 50 min; (D) ESI-MS spectrum of the extraction solution of porcine lung tissue obtained using CH_3OH/H_2O (v/v, 35/65) for 50 min; (E) iEESI-MS spectrum obtained by follow-up extraction using $CH_3OH/H_2O/CH_3COOH$ (v/v/v, 35/65/10); (F) ESI-MS spectrum of the extraction solution of porcine lung tissue obtained by follow-up extraction using $CH_3OH/H_2O/CH_3COOH$ (v/v/v, 35/65/10) for 1 min. (Note: (A), (C), and (E) in the left column are the mass spectra of iEESI-MS; (B), (D), and (F) in right column are the mass spectra of ESI-MS.)

blood of ovarian cancer and healthy volunteers[22] based on differences in amino acid and phospholipids metabolism, etc.), and environmental analysis (including quantification of 1-hydroxypyrene in raw human urine samples,[23] molecular characterization of particulate matters from gasoline cars,[24] and fast quantification of fluoroquinolones in environmental water samples,[25] etc.). A potential issue of this technique is that cells or smaller pieces of tissues may fall off during the analysis and contaminate the instrument. Also, contamination of the instrument is inevitable when large amounts of tissue samples were continuously analyzed over a long period of time. To address these problems, a disposable iEESI device which allowed precise sampling of defined-volume tissue samples (e.g., animal/plant tissue, etc.) with high reproducibility and accuracy was developed. The robustness of this sampling approach has been confirmed earlier.[16] Besides, the Figure S4 and Table S1 further indicated that the good reproducibility of iEESI-MS for tissue analysis. In future work, we will continue to improve the performance of the disposable iEESI device for the direct analysis of more types of real samples, including tissues, fluids, and cells.

Parameter Optimization. Owing to the unique extraction/ionization process occurring inside the inner part of a bulk sample, the intensity of ion signals in iEESI-MS showed a strong correlation with the chemical composition of the solution used for internal extraction of a bulk sample with multiple ingredients.[20] To screen the suitable solvents for favorable extraction/ionization of small metabolites, lipids and proteins originating from a single piece of human lung tissue sample, porcine lung tissue samples, which are readily available as a xenogeneic alternative to human lung for research purposes,[26] were chosen for parameter optimization. To explore solvents favorable for the extraction of small metabolites, a series of experiments were conducted using each newly loaded individual porcine lung tissue sample with different solvents including H_2O (Figure S2A), CH_3OH (Figure S2B), CH_3CH_2OH (Figure S2E), CH_3COOH (Figure S2D), and CH_3COCH_3 (Figure S3E). However, the mass spectra obtained with all solvents showed that only lipids in the mass range of m/z 700−900 and no small metabolites were acquired. Further, 21 extraction solutions composed of CH_3OH and H_2O at different ratios (0−100%) were also tested to achieve the best composition for extraction/ionization of lipids. As a result, the CH_3OH/H_2O (v/v, 35/65) solvent was chosen for iEESI-MS to profile lipids in the lung tissue, because the highest abundance and density of lipids were observed in the mass spectra. Interestingly, the chemical profiling of small metabolites was also obtained using the CH_3OH/H_2O (v/v, 35/65) solvent after continuous infusion for ca. 30−80 min. This might be related either to the exhaustion of lipids in tissue after ca. 30−80 min or to the degradation of lipids caused by oxidation at ambient conditions.[27,28] Note that the time required to exhaust lipids from the tissue sample varied dramatically from 30 to 80 min, depending on how much tissue material was loaded for the iEESI process. Similarly, signal levels of proteins were optimized once acetic acid was added to CH_3OH/H_2O (v/v, 35/65) at 10.0% (Figure S4). Consequently, the extraction solutions of CH_3OH/H_2O (v/v, 35/65) and $CH_3OH/H_2O/CH_3COOH$ (v/v/v, 35/65/10) were selected for sequential detection of lipids, small metabolites, and proteins in a single tissue sample.

Under the optimized conditions, distinctive mass spectrometric profiles of lipids (Figure 2A), small metabolites (Figure 2C), and proteins (Figure 2E) within a single porcine lung tissue sample were sequentially recorded using iEESI-MS with the specific solvents such as CH_3OH/H_2O (v/v, 35/65) and $CH_3OH/H_2O/CH_3COOH$ (v/v/v, 35/65/10). Note that lipids (Figure 2A) showed up at 1 min using CH_3OH/H_2O (v/v, 35/65), while small metabolites (Figure 2C) showed up after injection and were maintained stably for 50 min using the same solution. The lipids detected in the mass range of m/z 700−900 were tentatively identified as phosphatidylcholines (PCs), including m/z 757 $[PC(32:0) + Na]^+$, m/z 773 $[PC(32:0) + K]^+$, m/z 783 $[PC(36:4) + H]^+$, m/z 799 $[PC(34:1) + K]^+$, m/z 809 $[PC(36:2) + Na]^+$, and m/z 825

DOI: 10.1021/acs.analchem.9b01507
Anal. Chem. 2019, 91, 10532−10540

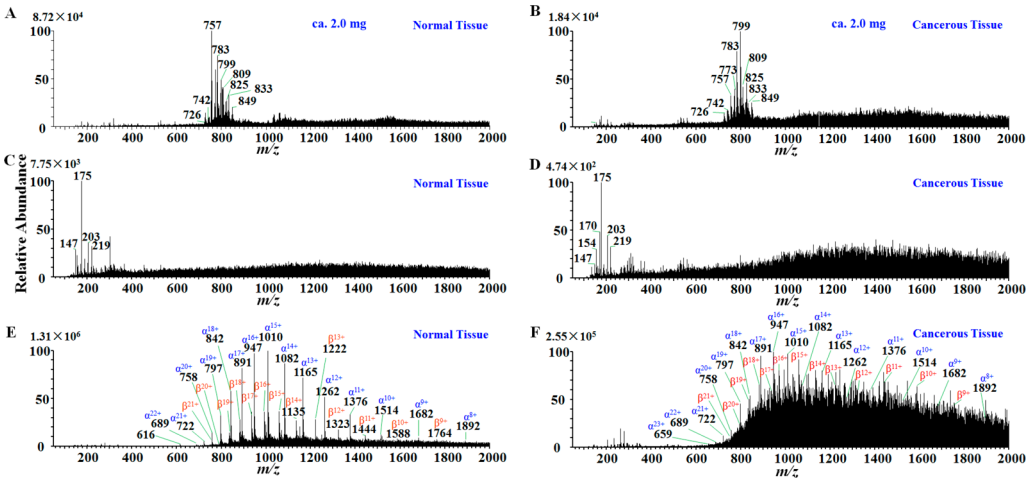

Figure 3. iEESI-MS of human lung tissue. (A, C) Mass spectra of normal tissue obtained using CH_3OH/H_2O (v/v, 35/65) as extractive solution for 1 and 80 min, respectively, (E) mass spectrum of normal tissue obtained using follow-up extraction by $CH_3OH/H_2O/CH_3COOH$ (v/v/v, 35/65/10) for 80 min, (B, D) mass spectra of cancerous tissue obtained using CH_3OH/H_2O (v/v, 35/65) as extractive solution for 1 and 70 min, respectively, and (F) mass spectrum of cancerous tissue obtained by follow-up extraction using $CH_3OH/H_2O/CH_3COOH$ (v/v/v, 35/65/10) for 70 min. (Note: (A), (C), and (E) in the left column are the mass spectra of normal tissue; (B), (D), and (F) in the right column are the mass spectra of cancerous tissue.)

$[PC(36:2) + K]^+$ using precision mass measurement and collision-induced dissociation (CID) data matching with the literature.[29−32] Accordingly, the small metabolites in the low mass range (m/z 100−250) (Figure 2C) were identified as m/z 132 $[Creatine + H]^+$, m/z 147 $[Glutamine + H]^+$, m/z 175 $[Arginine + H]^+$, m/z 203 $[Glucose + Na]^+$, and m/z 219 $[Glucose + K]^+$. Over the continuous infusion of the CH_3OH/H_2O (v/v, 35/65) solvent for 30−80 min, the MS signal decreased almost to the baseline, indicating that the lipids were exhausted. The mass spectrum was dominated by the signal of small metabolites in the mass range of m/z 100−250. Then, the protein signals (Figure 2E) were detected once the $CH_3OH/H_2O/CH_3COOH$ (v/v/v, 35/65/10) was infused as extractive solution without further hardware alteration. Clearly, the protein ions corresponding to α and β subunits of hemoglobin with wide charge state distributions (CSDs) in a relatively high mass range (m/z 600−1900) were detected (Figure 2E).[13,33] This further confirmed that the iEESI-MS technique is a solvent-dependent extraction process, which could be a potential tool for the sequential detection of lipids, small metabolites, and proteins in a single tissue sample.

For reference, the off-line extraction solution of a single porcine lung tissue sample (Figure S5) was analyzed by direct infusion electrospray ionization mass spectrometry (ESI-MS). As shown in Figure 2, the iEESI-MS mass spectra (Figure 2A, C, E in the left column) differed from the ESI-MS mass spectra (Figure 2B, D, F in the right column). For example, large amounts of the lipids, small metabolites, and proteins within a single bulk tissue were sequentially detected by iEESI-MS when the extraction solution was changed from CH_3OH/H_2O (v/v, 35/65) to $CH_3OH/H_2O/CH_3COOH$ (v/v/v, 35/65/10). On the other hand, no signal of lipids (Figure 2B) and small metabolites (Figure 2D) was obtained for the extraction solution of a single bulk tissue (ca. 2.0 mg) using CH_3OH/H_2O (v/v, 35/65) analysis by ESI-MS. Even when $CH_3OH/H_2O/CH_3COOH$ (v/v/v, 35/65/10) was used for extraction, only a low abundance ions of α and β subunits of hemoglobin were observed in ESI-MS (Figure 2F). The signal intensity of protein ions obtained in ESI-MS was about 2 orders of magnitude lower than that in iEESI-MS. We explain the difference in signal intensity of protein ions between iEESI-MS and ESI-MS by the fact that the volume of extraction solution (50 μL) used for off-line ESI-MS extraction was larger than that in on-line iEESI-MS extraction (less than 10 μL) for the tissue sample (ca. 2.0 mg). As a result, the amount of analyte in the electrospray solution for the direct infusion ESI-MS process is relatively lower than that for on-line iEESI-MS analysis. Alternatively, the inferior performance could also be attributed to other factors such as lower ionization efficiency and chemical interference in ESI-MS.[16] The ESI-MS spectra displayed strong background signal peaks at m/z 274 [*N*-lauryldiethanolamine + H]$^+$, m/z 279 [dibutyl phthalate + H]$^+$, and m/z 318 [*N*-(2-hydroxyethyl)-*N*-(2-(2-hydroxyethoxy)-ethyl) dodecylamine + H]$^+$, which are common MS contaminants.[34,35]

The direct comparison between iEESI-MS and conventional chromatographic approaches (such as liquid chromatography−mass spectrometry (LC-MS)/gas chromatography−mass spectrometry (GC-MS)) for the analysis of tissues was not undertaken in the present study. However, the direct comparison between iEESI-MS and conventional chromatographic approaches (LC-MS/GC-MS) for molecular quantification of bulk samples was performed in previous work on meat tissue samples. The results demonstrated that the limit-of-detection (LOD) values obtained using iEESI-MS were significantly lower than those obtained by conventional methods (GC-MS and LC-MS), probably due to the higher detection sensitivity by LTQ-MS instrument and higher ionization efficiency of iEESI-MS. The measured accuracy rates for iEESI-MS were in the range 92−105%.[16]

Possible Mechanism of Sequential Extraction of Lipids, Small Metabolites, and Proteins. Lipids are generally hydrophobic compounds,[5,36] which would float on the surface of the hydrophilic extraction solution of CH_3OH/H_2O (v/v, 35/65) used in iEESI-MS analysis. Thus, the signals of lipids were obtained prior to proteins and small metabolites. The solvent would gradually diffuse into bulk tissue sample over the time of iEESI analysis. Consequently, after the lipids

DOI: 10.1021/acs.analchem.9b01507
Anal. Chem. 2019, 91, 10532−10540

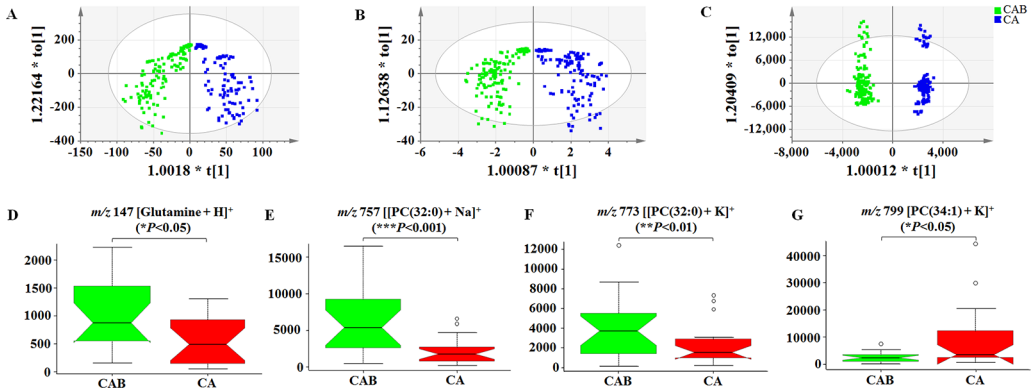

Figure 4. Statistical analysis of iEESI-MS data obtained with sequential extraction for the analysis of cancerous and normal tissues. Score plots of OPLS-DA of cancerous tissues (CA, blue squares) and normal tissues (CAB, green squares): (A) Small metabolites in the low mass range of m/z 100−250, (B) lipids in the mass range of m/z 700−900, and (C) proteins in the mass range of m/z 600−1900. Box plots of four selected peaks from Figure S8A, B with high VIP value: (D) m/z 147 $[\text{Glutamine} + \text{H}]^+$, (E) m/z 757 $[\text{PC(32:0)} + \text{Na}]^+$, (F) m/z 773 $[\text{PC(32:0)} + \text{K}]^+$, and (G) m/z 799 $[\text{PC(34:1)} + \text{K}]^+$. P values were determined with t test.

were exhausted over the continuous infusion of solvent CH_3OH/H_2O (v/v, 35/65) for ca. 30−80 min, the signal of small metabolites became dominant. Finally, intracellular proteins were extracted by using the $CH_3OH/H_2O/CH_3COOH$ (v/v/v, 35/65/10) solvent after cell lysis. Sequential extraction of lipids, small metabolites, and proteins in a single bulk tissue further indicated that iEESI-MS analysis is a solvent-dependent extraction process.

Direct Analysis of a Single Human Tissue Sample. A variety of ions were detected by iEESI-MS from either the normal lung tissue (Figure 3A, C, E in left column) or cancerous tissue (Figure 3B, D, F in right column). The predominant peaks at mass range of m/z 700−900 were identified as sphingomyelin (SM) and PCs, including m/z 726 $[\text{SM(34:1)} + \text{Na}]^+$, m/z 742 $[\text{SM(34:1)} + \text{K}]^+$, m/z 757 $[\text{PC(32:0)} + \text{Na}]^+$, m/z 773 $[\text{PC(32:0)} + \text{K}]^+$, m/z 783 $[\text{PC(36:4)} + \text{H}]^+$, m/z 799 $[\text{PC(34:1)} + \text{K}]^+$, m/z 809 $[\text{PC(36:2)} + \text{Na}]^+$, m/z 825 $[\text{PC(36:2)} + \text{K}]^+$, m/z 833 $[\text{PC(38:4)} + \text{Na}]^+$, and m/z 849 $[\text{PC(38:4)} + \text{K}]^+$, whereas peaks at mass range of m/z 100−250 included m/z 147 $[\text{Glutamine} + \text{H}]^+$, m/z 175 $[\text{Arginine} + \text{H}]^+$, m/z 203 $[\text{Glucose} + \text{Na}]^+$, and m/z 219 $[\text{Glucose} + \text{K}]^+$. Chemical assignment for the identified species from the tissue sample using iEESI-MS/MS is shown in Table S2, and the CID spectra of identified species are shown in Figure S6. Besides, peaks of α and β subunits of human hemoglobin with wide CSDs were evidently observed in the mass range of m/z 600−1900. The predominant compound assignments were based on high-resolution MS data, CID experiments, NIST/EPI/NIH Mass Spectral Library, and comparison with earlier literature data.[22,29−32] These results provide evidence that the established method could be used for the sequential detection of lipids, small metabolites, and proteins in a single bulk human tissue sample. By comparing the mass spectra of human tissue samples (Figure 3) with porcine lung tissue samples (Figure 2A, C, E), it was found that their mass spectra shared high consistency in the majority of main characteristic peaks with variations in relative abundance. This result indicated that porcine lung tissue samples are suitable to optimize parameters for the experiments on human lung tissues.

Note that the MS profiles recorded from the normal tissue samples were significantly different from those recorded using the cancer tissue samples. For example, the relative abundance of m/z 757 $[\text{PC(32:0)} + \text{Na}]^+$ in normal tissues was significantly increased compared with that in cancerous tissues (***P < 0.001), while the relative abundance of m/z 799 $[\text{PC(34:1)} + \text{K}]^+$ in cancerous tissues was significantly increased compared with that in normal tissues (*P < 0.05). Also, m/z 773 $[\text{PC(32:0)} + \text{K}]^+$ (**P < 0.01) was differentially expressed between cancerous and normal tissues; these results might indicate that PC species have different biological behaviors in the cancerous area.[31] Amino acids play an important role in carcinogenesis and are potential biomarkers in various cancers.[37,38] The signal intensity of m/z 147 $[\text{Glutamine} + \text{H}]^+$ was statistically significant between cancerous and normal tissues (*P < 0.05). The difference of m/z 147 $[\text{Glutamine} + \text{H}]^+$ in cancerous and normal tissues could be attributed to metabolically independent cancer cells and a five to ten times faster rate of glutamine consumption than normal cells.[39] Besides, the intensity of hemoglobin in normal tissues is higher than that in cancerous tissues. This might be related to the fact that the concentration of iron in cancerous tissue is significantly lower than in normal tissues,[40] and that lung tissue is highly vascularized to favor O_2/CO_2 exchanges.

Differential Analysis of Cancerous Tissues from Normal Tissues via OPLS-DA. To evaluate whether the molecular information obtained from human tissue samples by iEESI-MS is diagnostic and predictive of disease state,[41] the MS data obtained from a set of 48 tissue samples (including 24 cancerous tissue samples and 24 normal tissue samples) were subjected to OPLS-DA for differentiation of cancerous and normal tissue samples, seven data points for each tissue sample on average. As shown in Figure 4, the score plots of OPLS-DA based on small metabolites (Figure 4A), lipids (Figure 4B), and proteins (Figure 4C) exhibited a clear differentiation between cancerous and normal samples. This indicates that the multiple layers of molecular information obtained by iEESI-MS can be used to differentiate cancerous and normal tissues. For the OPLS-DA model of small metabolites (Figure 4A), the values of R^2X, R^2Y, and Q^2Y were 0.812, 0.728, and 0.689, respectively. For the OPLS-DA model of lipids (Figure 4B), the values of R^2X, R^2Y, and Q^2Y were 0.902, 0.824, and 0.65, respectively. For the OPLS-DA model of proteins (Figure 4C), the values of R^2X, R^2Y, and Q^2Y were 0.708, 0.982, and 0.912, respectively. Also, validation with 200 random permutation

DOI: 10.1021/acs.analchem.9b01507
Anal. Chem. 2019, 91, 10532−10540

tests of the PLS-DA model corresponding to the OPLS-DA model (Figure S7) generated intercepts R^2 = 0.225 and Q^2 = −0.564 for small metabolites (Figure S7A), R^2 = 0.358 and Q^2 = −0.444 for lipids (Figure S7B), and R^2 = 0.775 and Q^2 = −0.009 for proteins (Figure S7C), indicating that the models were not overfitted. Besides, S-plots (Figure S8) were constructed to screen for potential low molecular weight metabolite biomarkers, which displayed that small metabolites (Figure S8A) including m/z 147 $[Glutamine + H]^+$ and m/z 175 $[Arginine + H]^+$, lipids (Figure S8B) including m/z 757 $[PC(32:0) + Na]^+$, m/z 773 $[PC(32:0) + K]^+$, m/z 825 $[PC(36:2) + K]^+$, and m/z 849 $[PC(38:4) + K]^+$, and protein ions (Figure S8C) including m/z 758 (α^{+20}), m/z 797 (α^{+19}), m/z 842 (α^{+18}), m/z 883 (β^{+18}), m/z 891 (α^{+17}), m/z 935 (β^{+17}), m/z 947 (α^{+16}), m/z 993 (β^{+16}), m/z 1010 (α^{+15}), m/z 1082 (α^{+14}), and m/z 1165 (α^{+13}) were of high VIP value. This was further confirmed using t test analysis of individual potential biomarkers, box plots (Figure 4D−G) suggesting that the differences of these characteristic compounds, including m/z 147 $[Glutamine + H]^+$ (Figure 4D), m/z 757 $[PC(32:0) + Na]^+$ (Figure 4E), m/z 773 $[PC(32:0) + K]^+$ (Figure 4F), and m/z 799 $[PC(34:1) + K]^+$ (Figure 4G), were statistically significant between normal and cancerous tissues. These results further demonstrated that the established method could be applied to rapid differential analysis of cancerous and normal tissues at the molecular level.

Evaluation of Cancer Prediction Accuracy. Higher accuracy of cancer diagnosis will improve the patient's survival rate, ameliorate the cancer treatment strategy, and avert unnecessary biopsy.[42,43] To evaluate whether integrative molecular information at different layers could improve the cancer prediction accuracy, support vector machine (SVM), a kind of supervised learning model in machine learning, was applied to build a binary classification model.[43] The performance of the model was evaluated through the comparison of sensitivity, specificity, and accuracy of analysis (Table 1). With respect to the individual compound class analysis, the sensitivity, specificity, and accuracy obtained with integrative information on small metabolites and lipids for cancer prediction were improved from 54.0% to 67.0%, 51.0% to 100.0%, and 76.0% to 83.0%, respectively. The sensitivity and accuracy obtained with integrative information on small metabolites and proteins for cancer prediction were improved from 54.0% to 100.0% and 77.0% to 99.0%, respectively. Additionally, the sensitivity, specificity, and accuracy obtained with the integrative information on either small metabolites, lipids, and proteins or lipids and proteins for cancer prediction were substantially improved from 54.0%, 51.0%, and 76.0% to 100.0%, respectively. These results revealed that the integrative multilayers of molecular information could improve the cancer prediction accuracy. Therefore, the established method provides a new alternative diagnostic method for the accurate identification of the edges of pathogenic tissues. The open space for future research to further increase the accuracy of cancer differentiation by the iEESI-MS approach would be to use the negative polarity analysis in complement with the positive polarity analysis. This should allow higher molecular coverage and chemical specificity of differentiation.

Table 1. Cancer Prediction Results of Different Chemical Information Obtained Using SVM

Analytes	Sensitivity	Specificity	Accuracy
Metabolites	54.0%	100.0%	77.0%
Lipids	100.0%	51.0%	76.0%
Proteins	100.0%	98.0%	99.0%
Metabolites + Lipids	67.0%	100.0%	83.0%
Metabolites + Proteins	100.0%	98.0%	99.0%
Lipids + Proteins	100.0%	100.0%	100.0%
Metabolites + Lipids + Proteins	100.0%	100.0%	100.0%

Earlier experiments showed that lipids, small metabolites, and proteins from a single tissue sample could be simultaneously detected using $CH_3OH/H_2O/CH_3COOH$ (v/v/v, 35/65/2.5) (Figure S2F). Mass spectra of normal (Figure S9A) and cancerous (Figure S9B) tissue samples clearly showed that a variety of ions were detected by iEESI-MS using single extraction solution of $CH_3OH/H_2O/CH_3COOH$ (v/v/v, 35/65/2.5). The predominant peaks at mass range of m/z 100−250 included m/z 132 $[Creatine + H]^+$, m/z 175 $[Arginine + H]^+$, m/z 203 $[Glucose + Na]^+$, and m/z 219 $[Glucose + K]^+$. The signal peaks of phospholipids included m/z 757 $[PC(32:0) + Na]^+$, m/z 773 $[PC(32:0) + K]^+$, m/z 783 $[PC(36:4) + H]^+$, and m/z 799 $[PC(34:1) + K]^+$. Also, peaks of α and β subunits of hemoglobin with wide CSDs were evidently observed at higher mass range. To compare the performance of cancer prediction using integrative information on small metabolites, lipids, and proteins acquired with and without sequential extraction, the MS data (Figure S9) obtained from 9 tissue samples (including 4 normal tissue samples and 5 cancerous tissue samples) using single extraction solution of $CH_3OH/H_2O/CH_3COOH$ (v/v/v, 35/65/2.5) without sequential extraction were also analyzed for reference (Figure 5), seven data points for each tissue sample on average. The score plot of OPLS-DA (Figure 5A) showed that cancerous and normal tissue samples were clearly separated. Besides, the in-depth receiver operating characteristic (ROC) curve (Figure 5B) showed that the sensitivity,

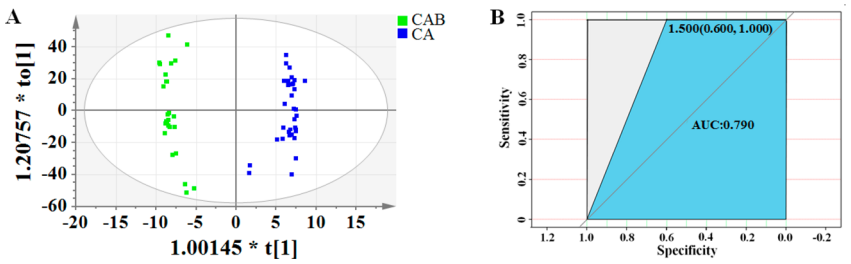

Figure 5. Statistical analysis of iEESI-MS data of cancerous and normal tissues obtained using single extraction solution of $CH_3OH/H_2O/CH_3COOH$ (v/v/v, 35/65/2.5) without sequential extraction. (A) Score plots of OPLS-DA of cancerous tissues (CA, blue squares) and normal tissues (CAB, green squares). (B) The ROC curve illustrates the performance of cancer prediction.

DOI: 10.1021/acs.analchem.9b01507
Anal. Chem. 2019, 91, 10532−10540

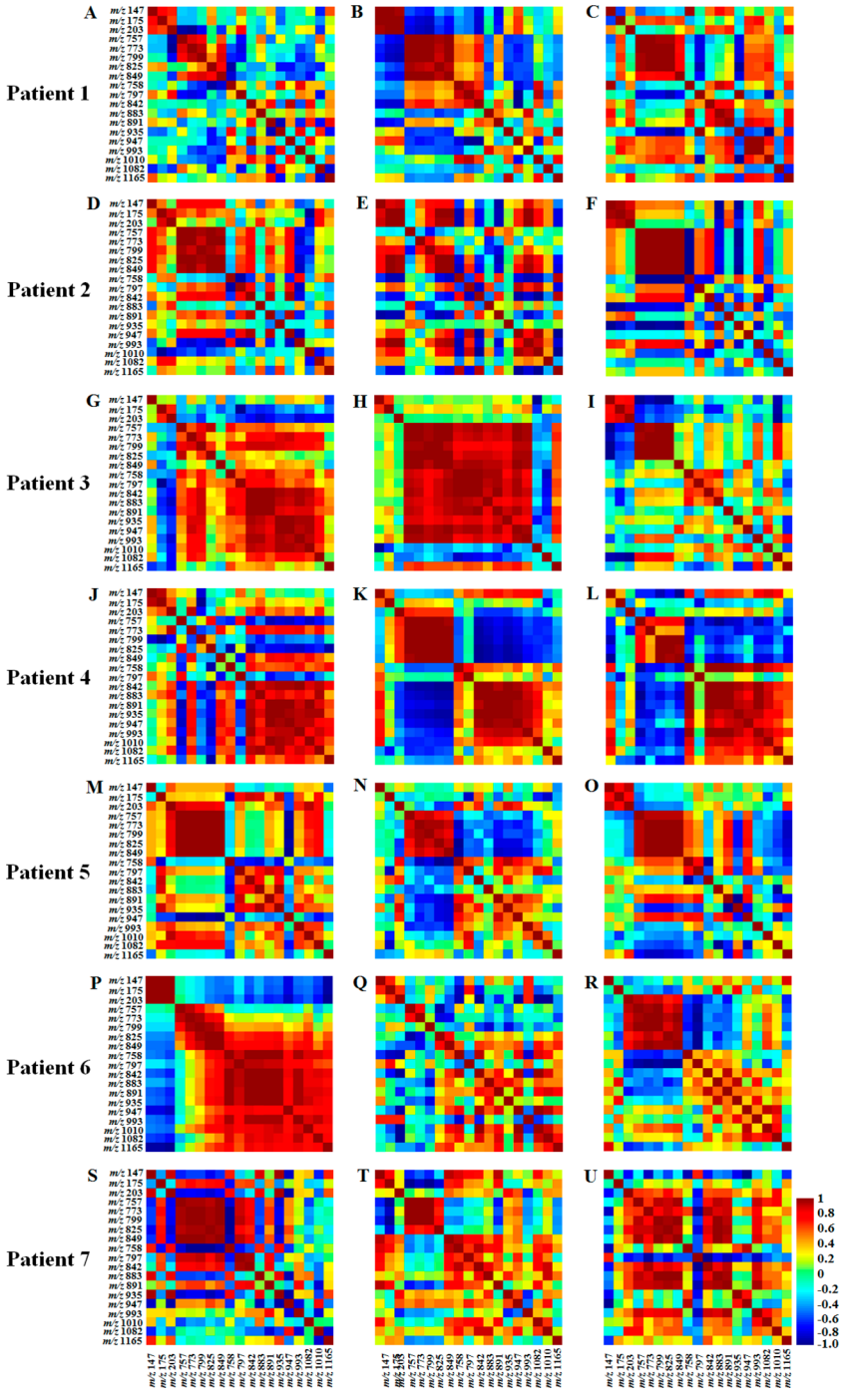

Figure 6. Correlation analysis of 19 signals with VIP of greater than 1.0 for the discrimination of cancerous and normal tissue samples. The 19 signals included small metabolites (including *m/z* 147, 175, and 203), lipids (including *m/z* 757, 773, 799, 825, and 849), and protein ions (including *m/z* 758, 797, 842, 883, 891, 935, 947, 993, 1010, 1082, and 1165). (A-C), (D-F), (G-I), (J-L), (M-O), (P-R), and (S-U) correspond to the correlation analysis of 19 compounds mentioned above in three individual tissue samples from patient 1, patient 2, patient 3, patient 4, patient 5, patient 6, and patient 7, respectively. Note: the gradient from green to red (the value range from 0 to 1) indicates that the positive correlation gradually increases. The gradient from green to blue (the value range from 0 to −1) indicates that the negative correlation gradually increases.

specificity, and area under the curve (AUC) obtained with the integrative information on small metabolites, lipids, and proteins for cancer prediction was 100.0%, 60.0%, and 79.0%, respectively. Apart from the sensitivity, the specificity (60.0%) and accuracy (79.0%) obtained without sequential extraction are significantly lower than the specificity (100.0%) and accuracy (100.0%) obtained with sequential extraction. These results indicate that integrative information on lipids, small metabolites, and proteins by the method with sequential extraction showed higher specificity and accuracy for cancer prediction.

Assessment of Systematic Error of Homologous Samples Analysis. For the OPLS-DA model, a variable influence on projection (VIP) is commonly used to summarize the importance of the variables to the model; variables with VIP of greater than 1.0 are considered to have differential

DOI: 10.1021/acs.analchem.9b01507
Anal. Chem. 2019, 91, 10532−10540

reliability and a statistically significant contribution to the model.[44,45] To assess the systematic error of homologous samples analysis, 19 signals (including small metabolites (e.g., m/z 147, 175, and 203) (VIP > 1.0), lipids (e.g., m/z 757, 773, 799, 825, and 849) (VIP > 1.0), and protein ions (e.g., m/z 758, 797, 842, 883, 891, 935, 947, 993, 1010, 1082, and 1165) (VIP > 5.0)) contributing to discrimination of cancerous and normal tissues were selected for correlation analysis. The result showed that even though a high degree of consistency was obtained among each individual tissue sample of the same specimen, with the range of correlation coefficients were 0.805 to 0.953 (Table S3), the relationship among small metabolites, lipids, and protein ions in three individual tissue samples showed no consistent patterns (Figure 6). Therefore, our results suggest that the outcomes of metabolomics, lipidomics, and proteomics acquired from each individual tissue sample might lead to the mismatch due to the systematic error of homologous samples analysis. In this regard, the ability of integrative analysis of multiple layers of molecular information from a single sample is desirable, as it can be helpful to reduce the systematic error of homologous samples analysis.

CONCLUSIONS

To conclude, sequential detection of lipids, small metabolites and proteins using exactly the same bulk tissue was demonstrated by iEESI-MS, requiring neither sample reloading nor instrumental hardware alteration. As demonstrated in this study, using 57 lung cancer samples of 13 patients, with respect to the individual compound class analysis, the sensitivity, specificity, and accuracy of the established strategy for cancer prediction were improved from 54.0%, 51.0%, and 76.0% to 100.0%, respectively, thus providing a novel analytical tool for advanced applications in precision molecular diagnosis and systems biology studies with minimized systematic errors, low sample consumption (ca. 2.0 mg), and simple operation.

ASSOCIATED CONTENT

Supporting Information

The Supporting Information is available free of charge on the ACS Publications website at DOI: 10.1021/acs.analchem.9b01507.

iEESI-MS experiment and working conditions; optimization of experimental conditions (including experimental parameters and extraction solutions); reproducibility test of iEESI-MS and ESI-MS experiments (PDF)

AUTHOR INFORMATION

Corresponding Authors

*E-mail: shfeng@jlu.edu.cn.
*E-mail: chw8868@gmail.com.

ORCID

Haiyan Lu: 0000-0003-2121-8212
Hua Zhang: 0000-0003-2875-7243
Yiping Wei: 0000-0002-5087-7113
Mufang Ke: 0000-0002-7137-4603
Keke Huang: 0000-0002-8995-2176
Shouhua Feng: 0000-0002-6967-0155

Notes

The authors declare no competing financial interest.

ACKNOWLEDGMENTS

This work was supported by the National Natural Science Foundation of China (Nos. 21727812, 21765001, 21565004, and 21427802), Science and Technology Planning Project at the Department of Science and Technology of Jiangxi Province, China (No. 20171ACG70015).

REFERENCES

(1) Surhone, L. M.; Timpledon, M. T.; Marseken, S. F. *Tissue (Biology)*; Betascript Publishing: 2010.
(2) Want, E. J.; Masson, P.; Michopoulos, F.; Wilson, I. D.; Theodoridis, G.; Plumb, R. S.; Shockcor, J.; Loftus, N.; Holmes, E.; Nicholson, J. K. *Nat. Protoc.* **2013**, *8*, 17−32.
(3) Li, T.; He, J.; Mao, X.; Bi, Y.; Luo, Z.; Guo, C.; Tang, F.; Xu, X.; Wang, X.; Wang, M.; Chen, J.; Abliz, Z. *Sci. Rep.* **2015**, *5*, 14089.
(4) Yuan, M.; Breitkopf, S. B.; Yang, X.; Asara, J. M. *Nat. Protoc.* **2012**, *7*, 872−881.
(5) Griffiths, W. J.; Wang, Y. *Chem. Soc. Rev.* **2009**, *38*, 1882−1896.
(6) De Vos, R. C.; Moco, S.; Lommen, A.; Keurentjes, J. J.; Bino, R. J.; Hall, R. D. *Nat. Protoc.* **2007**, *2*, 778−791.
(7) Eberlin, L. S.; Liu, X.; Ferreira, C. R.; Santagata, S.; Agar, N. Y.; Cooks, R. G. *Anal. Chem.* **2011**, *83*, 8366−8371.
(8) Sun, Y. V.; Hu, Y. J. *Adv. Genet.* **2016**, *93*, 147.
(9) Zhang, H.; Gu, H.; Yan, F.; Wang, N.; Wei, Y.; Xu, J.; Chen, H. *Sci. Rep.* **2013**, *3*, 2495.
(10) Zhang, H.; Zhu, L.; Luo, L.; Wang, N.; Chingin, K.; Guo, X.; Chen, H. *J. Agric. Food Chem.* **2013**, *61*, 10691−10698.
(11) Zhang, H.; Chingin, K.; Zhu, L.; Chen, H. *Anal. Chem.* **2015**, *87*, 2878−2883.
(12) Zhang, J.; Xu, J.; Ouyang, Y.; Liu, J.; Lu, H.; Yu, D.; Peng, J.; Xiong, J.; Chen, H.; Wei, Y. *Sci. Rep.* **2017**, *7*, 3738.
(13) Zhang, H.; Chingin, K.; Li, J.; Lu, H.; Huang, K.; Chen, H. *Anal. Chem.* **2018**, *90*, 12101−12107.
(14) Ma, T.; Fan, B. Y.; Zhang, C.; Zhao, H. J.; Han, C.; Gao, C. Y.; Luo, J. G.; Kong, L. Y. *Sci. Rep.* **2016**, *6*, 29926.
(15) Lu, H.; Zhang, H.; Zhou, W.; Chen, H. *Modern Food Sci. Technol.* **2016**, *32*, 298−303.
(16) Xu, J.; Xu, S.; Xiao, Y.; Chingin, K.; Lu, H.; Yan, R.; Chen, H. *Anal. Chem.* **2017**, *89*, 11252−11258.
(17) Lu, H.; Zhang, H.; Zhu, T.; Xiao, Y.; Xie, S.; Gu, H.; Cui, M.; Luo, L. *Sci. Rep.* **2017**, *7*, 5136.
(18) Song, L.; Xu, J.; Chingin, K.; Zhu, T.; Zhang, Y.; Tian, Y.; Chen, H.; Chen, X. *J. Agric. Food Chem.* **2017**, *65*, 7006−7011.
(19) Zhang, H.; Kou, W.; Bibi, A.; Jia, Q.; Su, R.; Chen, H.; Huang, K. *Sci. Rep.* **2017**, *7*, 14714.
(20) Lu, H.; Zhang, J.; Zhou, W.; Wei, Y.; Chen, H. *Chin. J. Anal. Chem.* **2016**, *44*, 329−334.
(21) Chagovets, V. V.; Wang, Z.; Kononikhin, A. S.; Starodubtseva, N. L.; Borisova, A.; Salimova, D.; Popov, I. A.; Kozachenko, A. V.; Chingin, K.; Chen, H.; Frankevich, V. E.; Adamyan, L. V.; Sukhikh, G. T. *Sci. Rep.* **2017**, *7*, 2546.
(22) Zhang, H.; Chingin, K.; Li, J.; Lu, H.; Huang, K.; Chen, H. *Anal. Chem.* **2018**, *90*, 12102−12107.
(23) Zhang, H.; Lu, H.; Huang, H.; Liu, J.; Fang, X.; Yuan, B.; Feng, Y.; Chen, H. *Anal. Chim. Acta* **2016**, *926*, 72−78.
(24) Zhang, H.; Li, Y.; Liu, K.; Zhu, L.; Chen, H. *Anal. Methods* **2017**, *9*, 6491−6498.
(25) Kou, W.; Zhang, H.; Bibi, A.; Ke, M.; Han, J.; Xiong, J.; Su, R.; Liang, D. *RSC Adv.* **2018**, *8*, 17293−17299.
(26) O'neill, J. D.; Anfang, R.; Anandappa, A.; Costa, J.; Javidfar, J.; Wobma, H. M.; Singh, G.; Freytes, D. O.; Bacchetta, M. D.; Sonett, J. R. *Ann. Thorac. Surg.* **2013**, *96*, 1046−1056.
(27) Wiswedel, I.; Gardemann, A.; Storch, A.; Peter, D.; Schild, L. *Free Radical Res.* **2010**, *44*, 135−145.
(28) Bochkov, V. N.; Oskolkova, O. V.; Birukov, K. G.; Levonen, A. L.; Binder, C. J.; Stoeckl, J. *Antioxid. Redox Signaling* **2010**, *12*, 1009−1059.

DOI: 10.1021/acs.analchem.9b01507
Anal. Chem. 2019, 91, 10532−10540

(29) Wang, H.; Manicke, N. E.; Yang, Q.; Zheng, L.; Shi, R.; Cooks, R. G.; Ouyang, Z. *Anal. Chem.* **2011**, *83*, 1197−1201.
(30) Wiseman, J. M.; Puolitaival, S. M.; Takats, Z.; Cooks, R. G.; Caprioli, R. M. *Angew. Chem. Int. Ed.* **2005**, *44*, 7094−7097.
(31) Guo, S.; Wang, Y.; Zhou, D.; Li, Z. *Sci. Rep.* **2015**, *4*, 5959.
(32) Morita, Y.; Sakaguchi, T.; Ikegami, K.; Goto-Inoue, N.; Hayasaka, T.; Hang, V. T.; Tanaka, H.; Harada, T.; Shibasaki, Y.; Suzuki, A. *J. Hepatol.* **2013**, *59*, 292−299.
(33) Hu, B.; Lai, Y. H.; So, P. K.; Chen, H.; Yao, Z. P. *Analyst* **2012**, *137*, 3613−3619.
(34) Chai, Y.; Chen, H.; Gao, G.; Liu, X.; Lu, C. *Rapid Commun. Mass Spectrom.* **2019**, *33*, 969−977.
(35) Keller, B. O.; Sui, J.; Young, A. B.; Whittal, R. M. *Anal. Chim. Acta* **2008**, *627*, 71−81.
(36) Holcapek, M.; Liebisch, G.; Ekroos, K. *Anal. Chem.* **2018**, *90*, 4249−4257.
(37) Song, Y.; Xu, C.; Kuroki, H.; Liao, Y.; Tsunoda, M. *J. Pharm. Biomed. Anal.* **2018**, *147*, 35−49.
(38) Bhutia, Y. D.; Babu, E.; Ramachandran, S.; Ganapathy, V. *Cancer Res.* **2015**, *75*, 1782−1788.
(39) Gul, K.; Mehmet, K.; Meryem, A. *Clin. Nutr.* **2017**, *36*, 1022−1028.
(40) Majewska, U.; Banas, D.; Braziewicz, J.; Gozdz, S.; Kubala-Kukus, A.; Kucharzewski, M. *Phys. Med. Biol.* **2007**, *52*, 3895−3911.
(41) Zhang, J.; Rector, J.; Lin, J. Q.; Young, J. H.; Sans, M.; Katta, N.; Giese, N.; Yu, W.; Nagi, C.; Suliburk, J. *Sci. Transl. Med.* **2017**, *9*, eaan3968.
(42) Gao, L.; Ye, M.; Lu, X.; Huang, D. *Genomics, Proteomics Bioinf.* **2017**, *15*, 389−395.
(43) Lan, H.; Duan, T.; Zhong, H.; Zhou, M.; Gao, F. *IEEE J. Sel. Top. Quantum Electron.* **2019**, *25*, 7201409.
(44) Booth, S. C.; Workentine, M. L.; Wen, J.; Shaykhutdinov, R.; Vogel, H. J.; Ceri, H.; Turner, R. J.; Weljie, A. M. *J. Proteome Res.* **2011**, *10*, 3190−3199.
(45) Galindo-Prieto, B.; Eriksson, L.; Trygg, J. *Chemom. Intell. Lab. Syst.* **2015**, *146*, 297−304.

DOI: 10.1021/acs.analchem.9b01507
Anal. Chem. 2019, 91, 10532−10540